eLIFE
elifesciences.org

Figures and figure supplements

MUL1 acts in parallel to the PINK1/parkin pathway in regulating mitofusin and compensates for loss of PINK1/parkin

Jina Yun, et al.

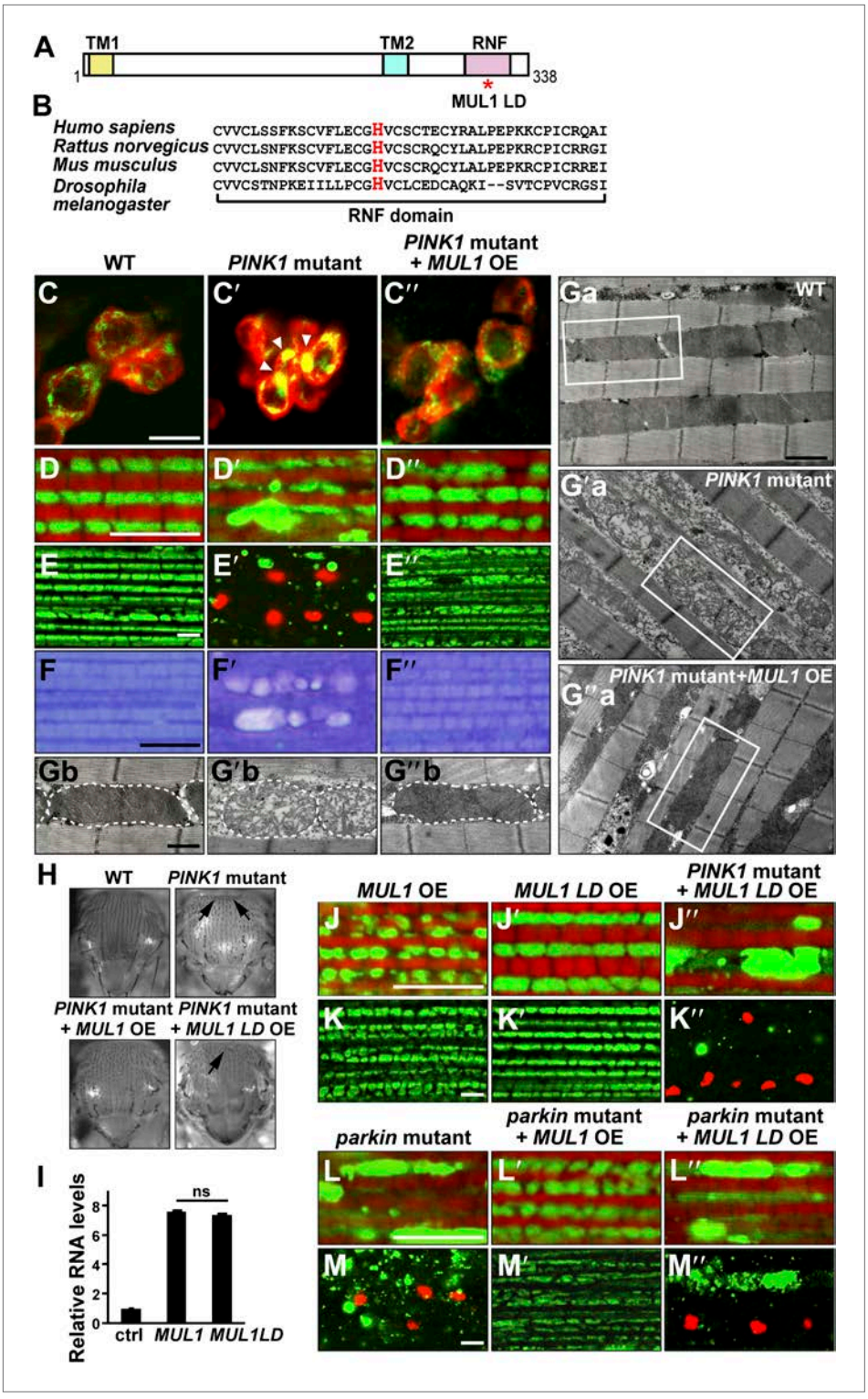

Figure 1. Overexpression of *MUL1*, but not *MUL1 LD*, suppresses *PINK1*/*parkin* mutant phenotypes. (**A**) Protein domain organization of Drosophila MUL1. TM1, TM2, and RNF represent transmembrane domains 1 and 2, and the RING Finger domain, respectively. The position of the mutation in the ligase dead (LD) version of MUL1 is marked with a red asterisk. (**B**) Sequence alignment of MUL1 in various species in the highly conserved RNF domain. A highly conserved histidine residue (marked as red) was mutated to alanine in MUL1 LD, ablating ligase activity. (**C**–**C**″) Dopaminergic neurons stained with an anti-TH antibody in red and mitochondria labeled with mitoGFP in

Figure 1. Continued on next page

Figure 1. Continued

green. Neurons in the PPL1 cluster are shown. While mitochondria in wild-type dopaminergic neurons are dispersed (**C**), mitochondria in *PINK1* mutant dopaminergic neurons are clumped (**C′**, white arrow heads). This phenotype is suppressed by *MUL1* overexpression driven by TH-Gal4 (**C″**). Scale bars: 10 μm. (**D**–**E″′** and **J**–**M″′**) Confocal images of the IFM from thoraces double labeled with mitoGFP and phalloidin (red) (**D**–**D″**, **J**–**J″**, **L**–**L″**), or double labeled with mitoGFP and TUNEL (red) with lower magnification (**E**–**E″**, **K**–**K″**, **M**–**M″**). Scale bars: 5 μm. *MUL1* overexpression is driven by Mef2-Gal4. In wild-type (**D**), mitochondria have a regular size and shape, and are localized in between myofibrils. In *PINK1* mutants (**D′**), mitochondrial size becomes irregular, and the GFP signal is reduced. Large mitochondrial clumps also appear. *PINK1* mutant muscle is TUNEL-positive (**E′**). (**F**–**F″**) Touidine blue staining of muscle. Compared with the wild-type (**F**), *PINK1* mutant muscle shows vacuolation indicating muscle degeneration (**F′**). These *PINK1* mutant phenotypes (**D′**, **E′**, **F′**) are almost completely suppressed by *MUL1* overexpression (**D″**, **E″**, **F″**). (**Ga**–**Ga″**, **Gb**–**Gb″**) EM images of mitochondria in muscle. (**Gb**–**Gb″**) Single mitochondrion (outlined with dashed lines) from white boxes in **Ga**–**Ga″**. Scale bars: 1 μm (**Ga**–**G″a**) 0.5 μm (**Gb**–**G″b**). In wild-type (**Ga** and **Gb**), mitochondria have compact and organized cristae whereas mitochondria from *PINK1* mutants (**Ga′**, **Gb′**) are swollen with fragmented cristae, and this is rescued by *MUL1* overexpression (**Ga″**, **Gb″**). (**H**) Images of thoraces. Arrows point to thoracic indentations due to muscle degeneration. Compared with WT, *PINK1* mutants have thoracic indentation due to muscle degeneration. *MUL1* overexpression, but not *MUL1 LD* overexpression, suppresses *PINK1* mutant thoracic indentation. (**I**) qPCR analysis shows that *MUL1* and *MUL1 LD* mRNA are expressed at similar levels in muscles. The data are shown as the mean ± SEM from three experiments (RNA from ten 5-day-old fly thoraces for each genotype). The statistical analysis was done using One-way ANOVA with Tukey' multiple comparisons test. ns: not statistically significant. *MUL1 LD* overexpression in the *PINK1* mutant background does not suppress the formation of mitochondrial clumps (**J″**) or TUNEL-positivity (**K″**). (**L**–**M″**) Overexpression of *MUL1*, but not *MUL1 LD*, suppresses *parkin* mutant phenotypes.

DOI: 10.7554/eLife.01958.003

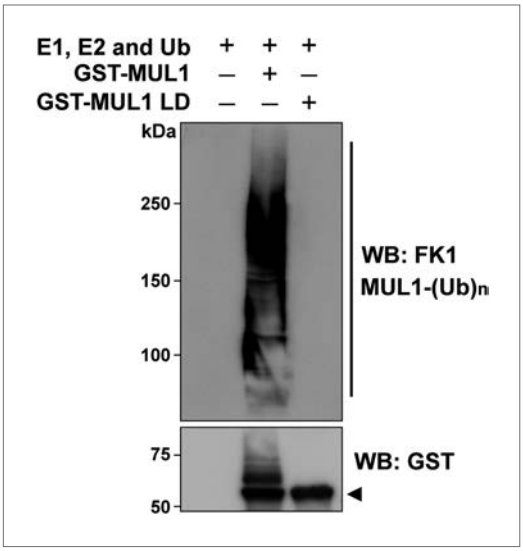

Figure 1—figure supplement 1. MUL1, but not its ligase-dead version (MUL1 LD), is able to self-ubiquitinate in vitro.

DOI: 10.7554/eLife.01958.004

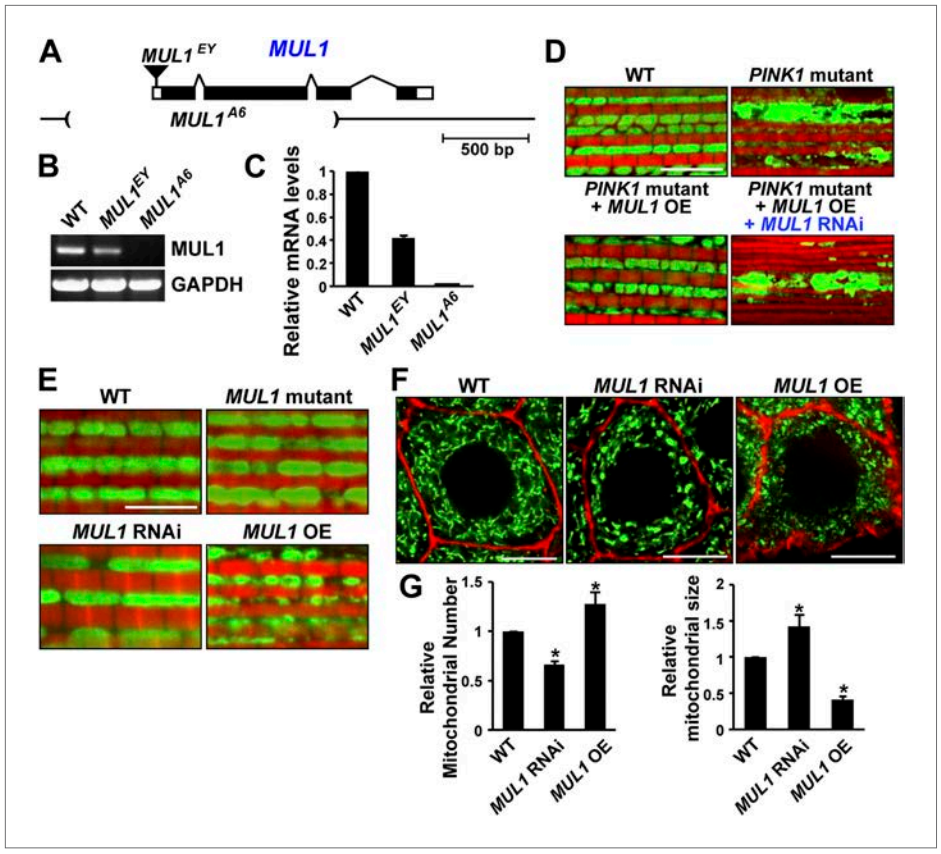

Figure 2. *MUL1* regulates mitochondrial morphology. (**A**) A schematic depicting the Drosophila *MUL1* genomic region (cytological location 64A4). *MUL1* coding and untranslated regions (dark and open rectangles, respectively) are depicted. The P element, $MUL1^{EY}$, inserted in the 5′ UTR, is shown as an inverted triangle. The deleted region in the $MUL1^{A6}$ allele is indicated by parentheses. (**B**) RT PCR shows that flies carrying the $MUL1^{EY}$ allele have detectable but reduced levels of *MUL1* transcripts. However, no *MUL1* transcript is detected in flies homozygous for the *MUL1* deletion, $MUL1^{A6}$. (**C**) qPCR shows that $MUL1^{EY}$ allele has approximately a 60% reduction of *MUL1* transcript compared to the wild-type (WT). No *MUL1* transcript is detected in flies homozygous for $MUL1^{A6}$. (**D**) *MUL1* RNAi line reverses the suppression of *PINK1* mutant mitochondrial phenotypes due to *MUL1* overexpression. (**E**) Muscle fibers stained with mitoGFP in green and actin in red. Compared with the WT, flies homozygous for the *MUL1* deletion or expressing *MUL1* RNAi show slightly elongated mitochondria. In contrast, when *MUL1* is overexpressed using the Mef2-Gal4 driver, mitochondria are significantly smaller. (**F**) Salivary glands, with cell boundaries labeled with rhodamine phalloidin in red, and mitoGFP in green. In WT, mitochondria are tubular and evenly distributed. In contrast, in cells expressing *MUL1* RNAi (driven by OK6-Gal4) mitochondria are fewer in number and found in clumps. In contrast, *MUL1* overexpression (also driven by OK6-Gal4) results in fragmented mitochondria and irregular cell boundaries. (**G**) Quantification of mitochondrial number and size in salivary glands (mean ± SEM, n > 6 larvae for each genotype). * Significantly different from wild-type, $p<0.05$ (One-way ANOVA with Tukey's multiple comparisons test).
DOI: 10.7554/eLife.01958.005

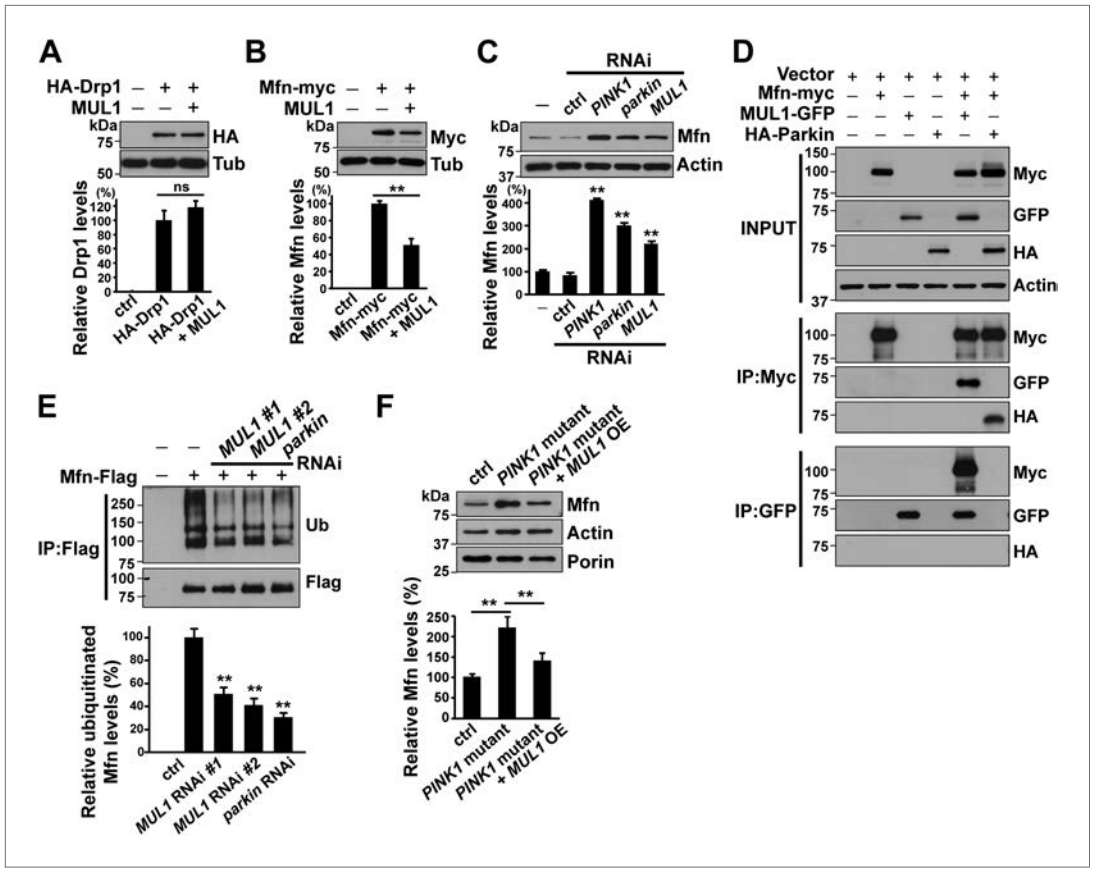

Figure 3. MUL1 physically binds to Mfn, and promotes ubiquitination-mediated Mfn degradation. (**A** and **B**) Western blots and quantifications of Drp1 and Mfn levels in vivo. Analysis of lysates from thoraces show that *MUL1* overexpression reduces Mfn levels (**B**) but not Drp1 levels (**A**). The data are shown as the mean ± SEM from three experiments (each experiment was done with lysate from 8 thoraces for each genotype). The statistical analysis was done using One-way ANOVA with Tukey's multiple comparisons test. ns: not statistically significant. ** Significantly different, p<0.01. (**C**) Western blots of Mfn levels in S2 cells either not treated or treated with control, *PINK1*, *parkin* or *MUL1* RNAi. Quantification of relative Mfn levels shows that there is an increase in Mfn levels in cells treated with RNAi to *PINK1*, *parkin*, or *MUL1* (mean ± SEM, ** Significantly different from cells not treated with RNAi, p<0.01, One-way ANOVA with Tukey's multiple comparisons test). (**D**) Co-immunoprecipitation using lysates from S2 cells transfected with the indicated constructs. The INPUT represents 2% of total lysate to monitor protein expression (top panel). MUL1-GFP is co-immunoprecipitated with Mfn-myc using both anti-GFP and anti-Myc antibodies. Mfn-myc also co-immunoprecipitates with HA-Parkin, which serves as a positive control. The interaction between Mfn-Myc and MUL1-GFP was specific, as confirmed by separate immunoprecipitation control experiments (***Figure 3—figure supplement 1***). (**E**) Mfn ubiquitination levels in S2 cells. S2 cells are treated with dsRNA designed to silence various genes and transfected with Mfn-Flag. Immunoprecipitation was performed with anti-Flag antibody, and Western blots were probed with anti-Ubiquitin antibody and an anti-Flag antibody. Relative ubiquitination levels compared to control are shown below (mean ± SEM). ** Significantly different from control, p<0.01 (One-way ANOVA with Tukey's multiple comparisons test). In S2 cells, Mfn is highly ubiquitinated. RNAi of *MUL1* or *parkin* results in reduced levels of ubiquitnated Mfn. Two independent *MUL1* RNAs are utilized to knockdown *MUL1*, which yield the same results. (**F**) In *PINK1* mutant thoraces, where Mfn levels are increased, *MUL1* overexpression (driven by Mef2-Gal4) reduces the increased Mfn levels. Relative Mfn levels compared to control are shown below (mean ± SEM). ** Significantly different, p<0.01 (One-way ANOVA with Tukey's multiple comparisons test).

DOI: 10.7554/eLife.01958.006

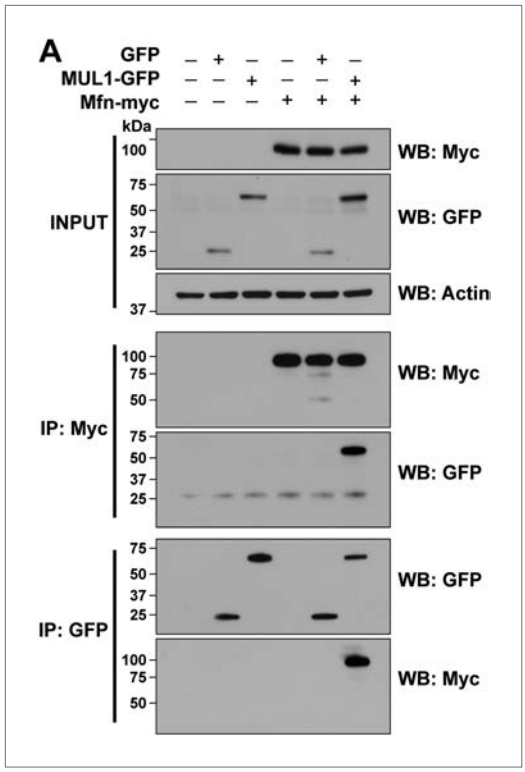

Figure 3—figure supplement 1. MUL1 co-immunoprecipitates with Mfn in S2 cells.

DOI: 10.7554/eLife.01958.007

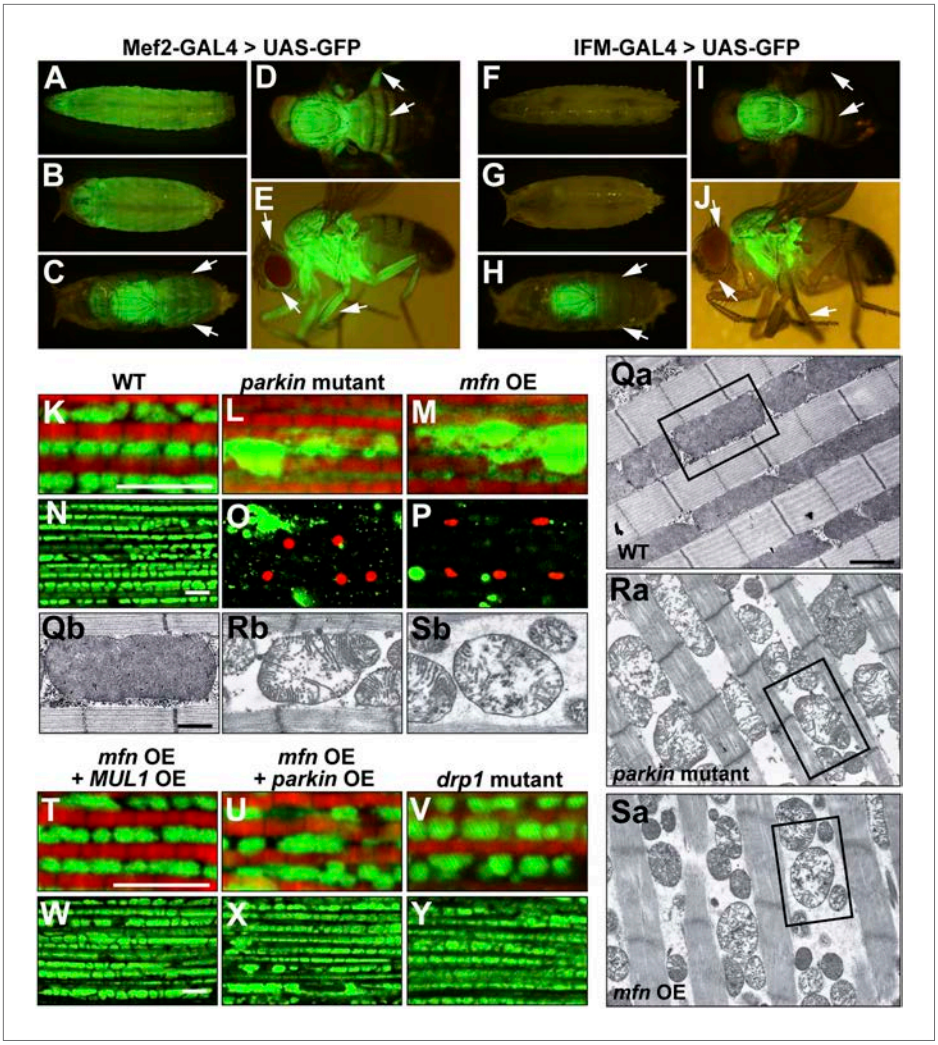

Figure 4. Generation and expression of the IFM-GAL driver; *mfn* overexpression, but not loss of *drp1*, induces *PINK1/parkin*-mutant like pathology. (**A**–**J**) Different developmental stages of flies expressing GFP under Mef2-Gal4 (**A**–**E**) or IFM-Gal4 (**F**–**J**). (**A**) Third instar larvae show GFP expression in whole body muscles. (**B**) At the early pupal stage, GFP is expressed in a similar pattern as in larvae. However, the GFP expression pattern become more specific at the late pupal stage (**C**), in which the strongest GFP signal is seen in the thorax, and a weaker signal is observed in the head and abdomen (arrows). (**D**) In an adult fly, dorsal view shows GFP signal in the thorax, upper abdomen and legs. (**E**) GFP is also expressed in adult head and legs, marked with arrows. (**F**) Flies expressing GFP under IFM-Gal4 show no GFP expression in third instar larvae, or in early pupae (**G**). (**H**) GFP is strongly expressed only in the thorax at the late pupal stage, but not in other areas (arrows). (**I**) In the adult fly, GFP signal is highly concentrated in the thorax. No GFP expression in abdomen and legs is observed, arrows. (**J**) In contrast to GFP expression under Mef2-Gal4, IFM-Gal4 does not express in adult head or legs, as indicated with arrows. (**K**–**P**, **T**–**Y**) Confocal images of muscle double labeled with mitoGFP (green) and phalloidine (red) (**K**–**M**, **T**–**V**), or those labeled with mitoGFP and TUNEL (red) at lower magnification (**N**–**P**, **W**–**Y**), respectively. (**Qa**–**Sb**) EM images of mitochondria in muscle. Single mitochondrion from the black-boxed area in **Qa**, **Ra**, **Sa** is shown in Qb, Rb, Sb. Scale bars: 1 μm (**Qa**, **Ra**, **Sa**) and 0.5 μm (**Qb**, **Rb**, **Sb**). Compared with wild-type (**K** and **N**), *parkin* null mutant (**L** and **O**) shows overall reduced levels of mitoGFP signal, large mitochondrial clumps, and muscle cell death. Similar phenotypes are observed with *mfn* overexpression (**M** and **P**), and these phenotypes are suppressed by *MUL1* overexpression (**T** and **W**). As a control, *parkin* overexpression also suppresses phenotypes due to *mfn* overexpression (**U** and **X**). Importantly, *drp1* null ($drp1^{1}/drp1^{2}$) mutant muscle does not have any mitochondrial clumping or TUNEL-positivity seen in loss of *parkin* function or *mfn* overexpression (**V** and **Y**). *mfn* overexpression is driven by IFM-Gal4. Scale bars: 5 μm.

DOI: 10.7554/eLife.01958.008

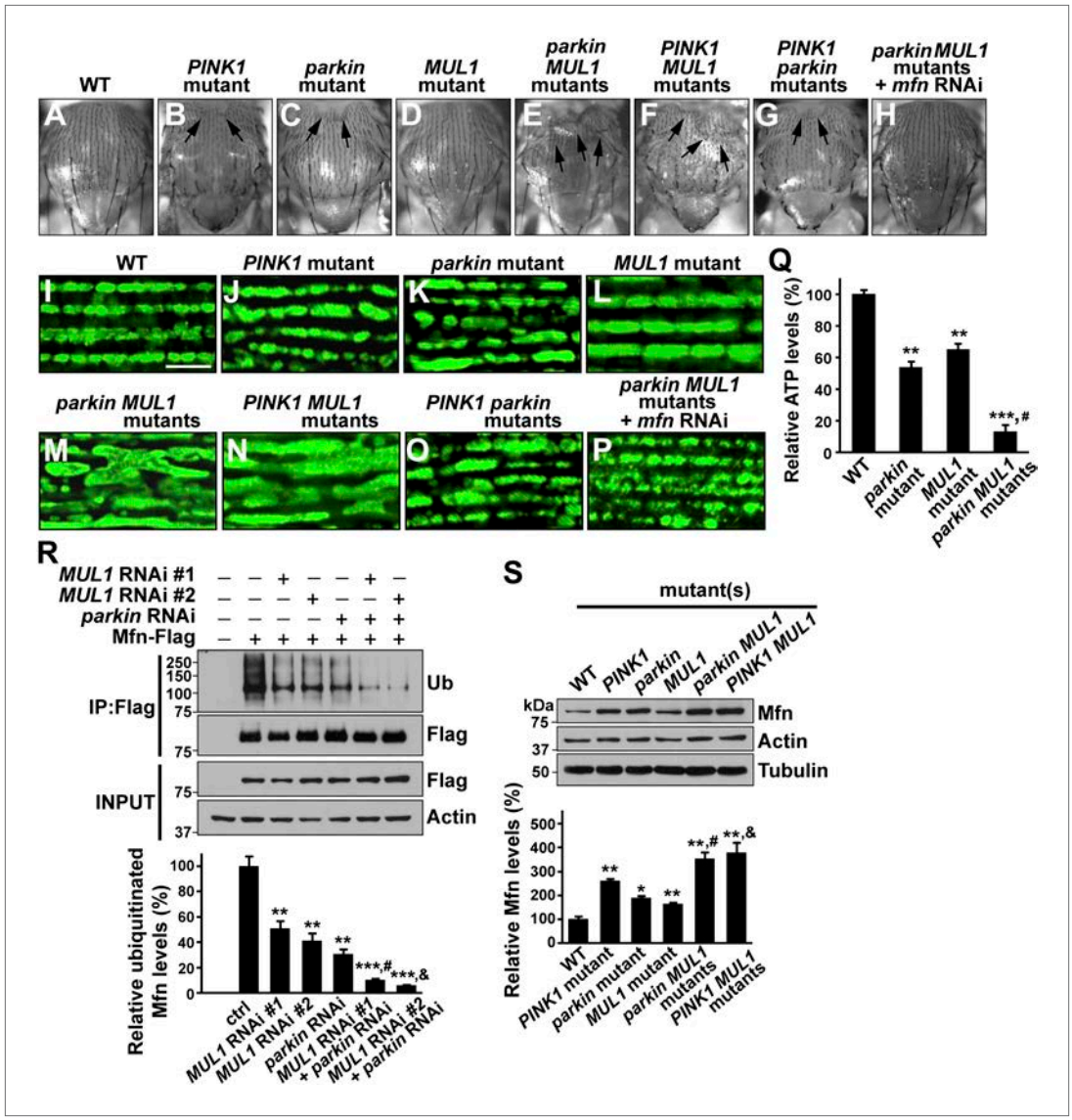

Figure 5. *MUL1* acts in parallel to the PINK1/parkin pathway. (**A**–**H**) Images of thoraces of various mutants. Arrows point to thoracic indentations due to muscle degeneration. *PINK1 MUL1* and *parkin MUL1* double mutants have more severe thoracic indentation compared to either mutant alone. Remarkably, the severe thoracic indentation phenotype in *parkin MUL1* double mutants is almost completely suppressed when *mfn* is also knocked down. (**I**–**P**) Mitochondria are labeled using an anti-ATP synthase antibody in the IFM. While *PINK1*, *parkin*, and *MUL1* mutant show slightly elongated mitochondrial morphology, *PINK1 MUL1* and *parkin MUL1* double mutants exhibit highly elongated and interconnected mitochondria. These phenotypes can be suppressed by *mfn* knockdown. Instead of using mitoGFP, we utilized anti-ATPase antibodies that allow better visualization of the enhancement phenotypes seen with double mutants. (**Q**) Relative ATP levels in whole flies of various mutants (mean ±SEM from three experiments, five 5-day-old flies for each genotype). ** and *** significantly different from wild-type, $p<0.01$ and $p<0.001$, respectably (One-way ANOVA with Tukey's multiple comparisons test). # Significantly different from *parkin* mutant and *MUL1* mutant, both $p<0.01$ (Two-way ANOVA with Tukey's multiple comparisons test). (**R**) In vivo ubiquitination assay of Mfn. S2 cells were treated with the indicated RNAi, transfected with Flag-Mfn, and treated with proteasome inhibitor MG132. Immunoprecipitations were performed using anti-Flag antibody, and western blots were probed with antibodies against anti-Ubiquitin antibody (P4D1) or anti-Flag antibody. Relative ubiquitination levels compared to control are shown in the lower panel (mean ± SEM). ** and *** Significantly different from control, $p<0.01$ and $p<0.001$, respectably (One-way ANOVA with Tukey's multiple comparisons test). # Significantly different from *MUL1* RNAi #1 and *parkin* RNAi, both $p<0.01$. & Significantly different from *MUL1* RNAi #2 and *parkin* RNAi, $p<0.001$ and $p<0.01$, respectably (Two-way ANOVA with Tukey's multiple comparisons test). (**S**) Western

Figure 5. Continued on next page

Figure 5. Continued

blot analysis of Mfn levels in vivo and quantification (mean ± SEM from three experiments, eight third instar larvae for each genotype). * and ** significantly different from wild-type, $p<0.05$ and $p<0.01$, respectably (One-way ANOVA with Tukey's multiple comparisons test). # Significantly different from *parkin* mutant and *MUL1* mutant, both $p<0.01$. & Significantly different from *PINK1* mutant and *MUL1* mutant, both $p<0.01$ (Two-way ANOVA with Tukey's multiple comparisons test).

DOI: 10.7554/eLife.01958.009

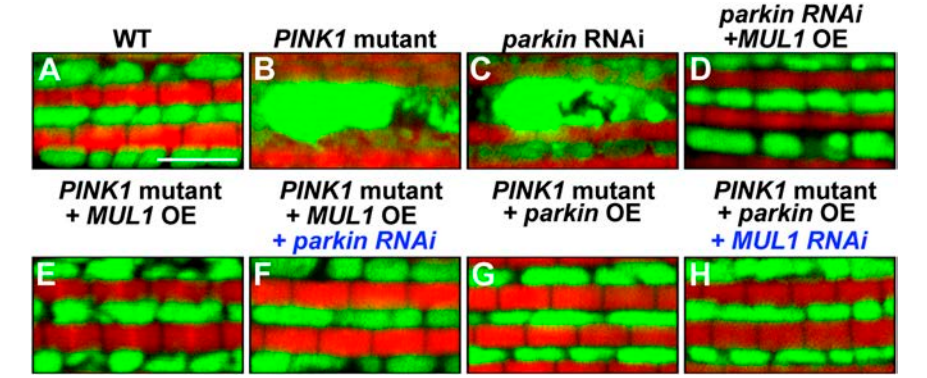

Figure 5—figure supplement 1. *MUL1* acts in a parallel pathway to the *PINK1/parkin* pathway.

DOI: 10.7554/eLife.01958.010

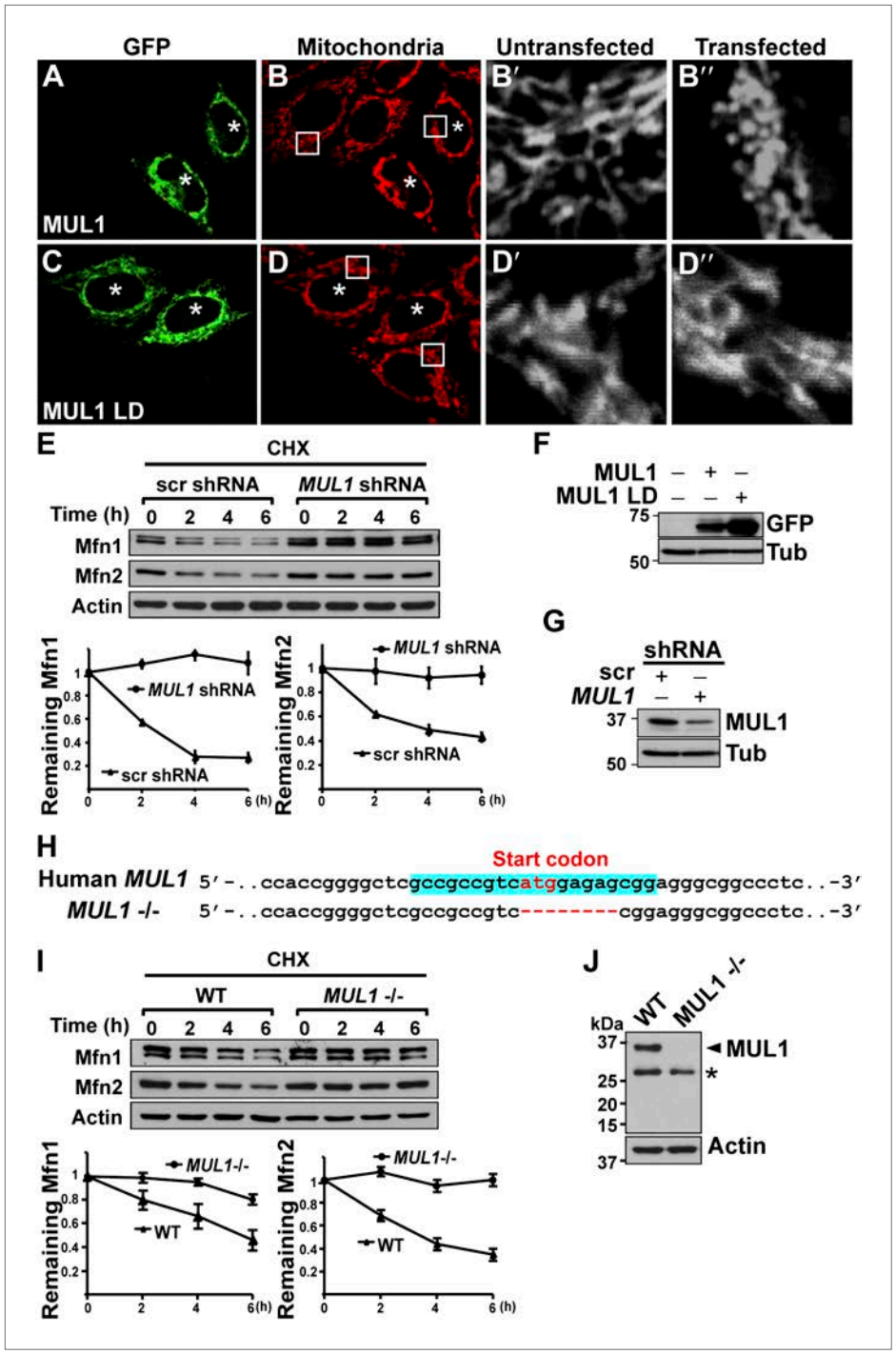

Figure 6. *MUL1*'s function in mitochondrial morphology and Mfn levels is conserved in human cells. (**A**–**D**‴) HeLa cells transfected with GFP-MUL1 (**A**–**B**″) or GFP-MUL1 LD (**C**–**D**″) are marked with asterisks, while cells not transfected serve as internal controls. Mitochondria are labeled with mitotracker in red (**B** and **D**). (**B**′ and **B**″, **D**′ and **D**″) Higher magnification images of mitochondria within white boxes in **B** and **D**. Cells expressing GFP-MUL1 have clustered mitochondria in the perinuclear region (**B**). Mitochondria are also small and fragmented (**B**″), as compared to cells not expressing GFP-MUL1 (**B**′). Importantly, GFP-MUL1 LD does not result in localization of mitochondria to the perinuclear region (**D**) or in mitochondrial fragmentation (**D**′). (**E**) Western blot analysis of Mfn1 and Mfn2 levels after CHX treatment. HeLa cells expressing scrambled shRNA or *MUL1* sh*MUL1* are treated with CHX. Mfn1 and 2 levels at each time point are normalized with Actin. The relative portion of remaining Mfn1 and 2 as compared to time point 0 was calculated and plotted (**E**). In cells expressing *MUL1* shRNA, Mfn1 and 2 levels after CHX

Figure 6. Continued on next page

Figure 6. Continued

treatment are more stable than those in cells expressing scrambled shRNA. (**F**) Expression of transfected GFP-MUL1 and GFP-MUL1 LD in HeLa cells, as detected using anti-GFP antibody. (**G**) Western blot analysis of endogenous MUL1 levels in HeLa cells stably expressing scrambled shRNA and *MUL1* shRNA. *MUL1* shRNA expressing cells have reduced levels of endogenous MUL1. (**H**) Human *MUL1* sequence and deletion in *MUL1* knockout (*MUL1*−/−) HeLa cells, generated using the CRISPR/Cas 9 system. Sequences targeting *MUL1* are highlighted in blue. Red letters indicate start codon. Red dashes represent deleted bases. Deleted eight base pairs include the start codon of MUL1. (**I**) Western blot analysis of Mfn1 and Mfn2 levels in wild-type and *MUL1*−/− HeLa cells treated with CHX for the indicated time. Remaining Mfn1 and Mfn2 levels at each time point were plotted below. (**J**) Western blot showing no MUL1 expression in *MUL1*−/− HeLa. Arrowhead points to MUL1 protein. Asterisk indicates a non-specific band.

DOI: 10.7554/eLife.01958.011

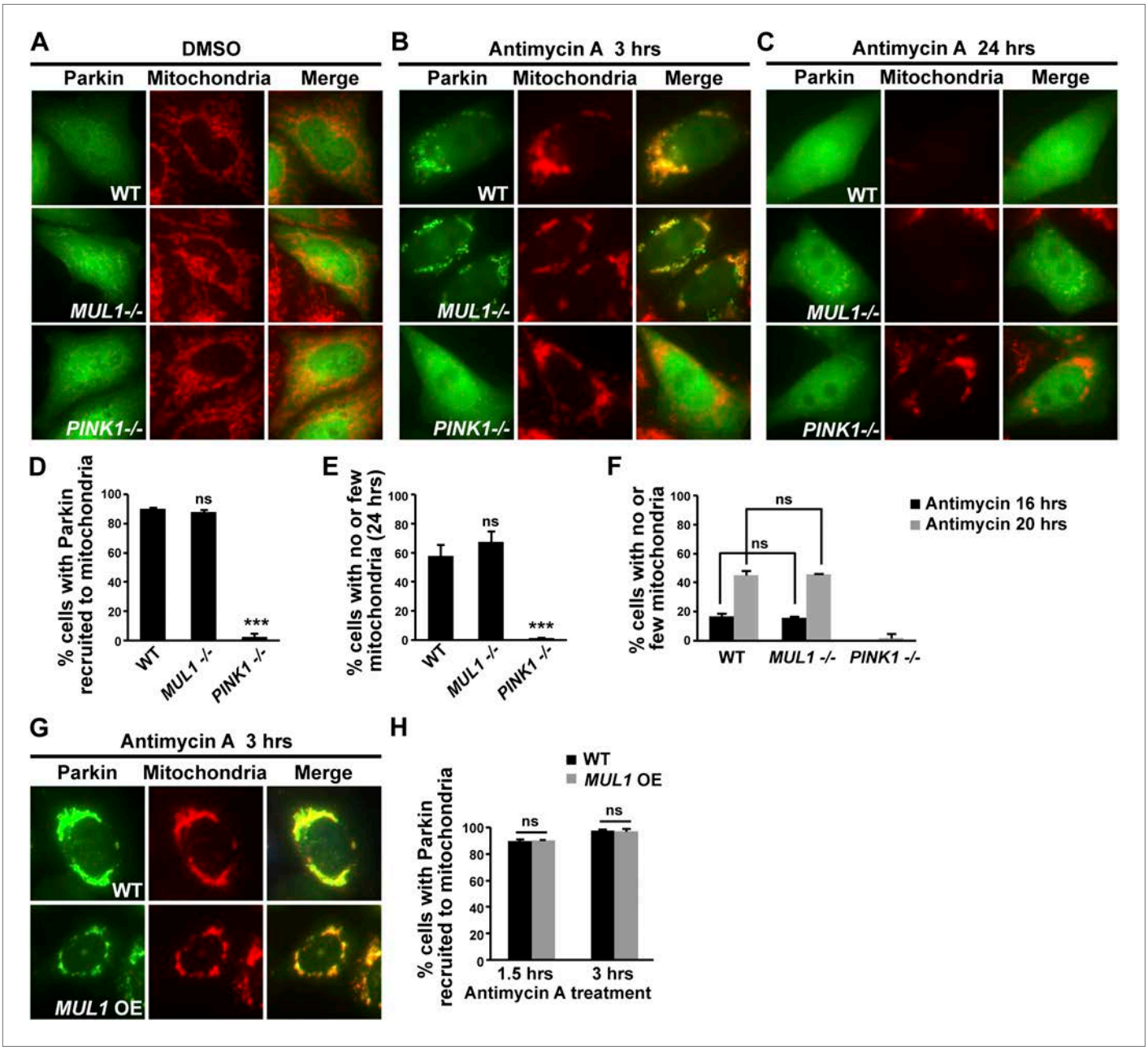

Figure 7. Neither *MUL1* knockout nor overexpression affects Parkin-mediated mitophagy. (**A**–**C**) HeLa cells (control, *MUL1* knockout or *PINK1* knockout) were transfected with YFP-Parkin, treated with either DMSO or antimycin A, and immunostained with an anti-Tom20 antibody which labels mitochondria. (**A**) HeLa cells treated with DMSO as a control. (**B**) Following treatment with antimycin A for 3 hrs, Parkin is recruited to mitochondria, as shown by co-localization of Parkin and the mitochondrial marker. In *MUL1* null cells, Parkin recruitment to mitochondria is not affected, whereas in *PINK1* null cells (positive control), Parkin recruitment to mitochondria is abolished. (**C**) After 24 hrs of antimycin A treatment, Parkin returns to the cytosol and the mitochondrial signal disappears. In *MUL1* null cells, mitochondrial disappearance occurs similarly as with WT, whereas in *PINK1* null cells (positive control), mitochondria are not eliminated. (**D**–**E**) Quantification of cells with Parkin recruited to mitochondria after 3 hrs of antimycin A treatment (**D**) and with few or no mitochondria after 24 hr of antimycin A treatment (**E**) and after 16 and 20 hrs of antimycin A treatment (**F**). The data are shown as the mean ± SEM from three experiments (n ≥ 100 for each genotype). *** Significantly different from wild-type, $p<0.001$. ns: not statistically significant (One-way ANOVA with Tukey's multiple comparisons test). While Parkin translocation and mitochondrial disappearance are significantly blocked in *PINK1* knockout cells, there is no significant difference between HeLa cells and *MUL1* knockout cells in these processes. (**G**) HeLa cells stably expressing YFP-Parkin and mito-RFP are transfected with Flag-MUL1, treated with DMSO or antimycin A, and immunostained with anti-Flag antibody. 3-hour antimycin A treatment causes Parkin localization to mitochondria in cells with or without *MUL1* expression. (**H**) Quantification of cells with Parkin recruited to mitochondria after 1.5 or 3 hrs Antimycin A treatment. Both 1.5 and 3 hrs of antimycin A treatments results in similar levels of Parkin

Figure 7. Continued on next page

Figure 7. Continued

recruitment to mitochondria. The data are shown as the mean ± SEM from three experiments (n ≥ 100 for each genotype). ns: not statistically significant (One-way ANOVA with Tukey's multiple comparisons test).

DOI: 10.7554/eLife.01958.012

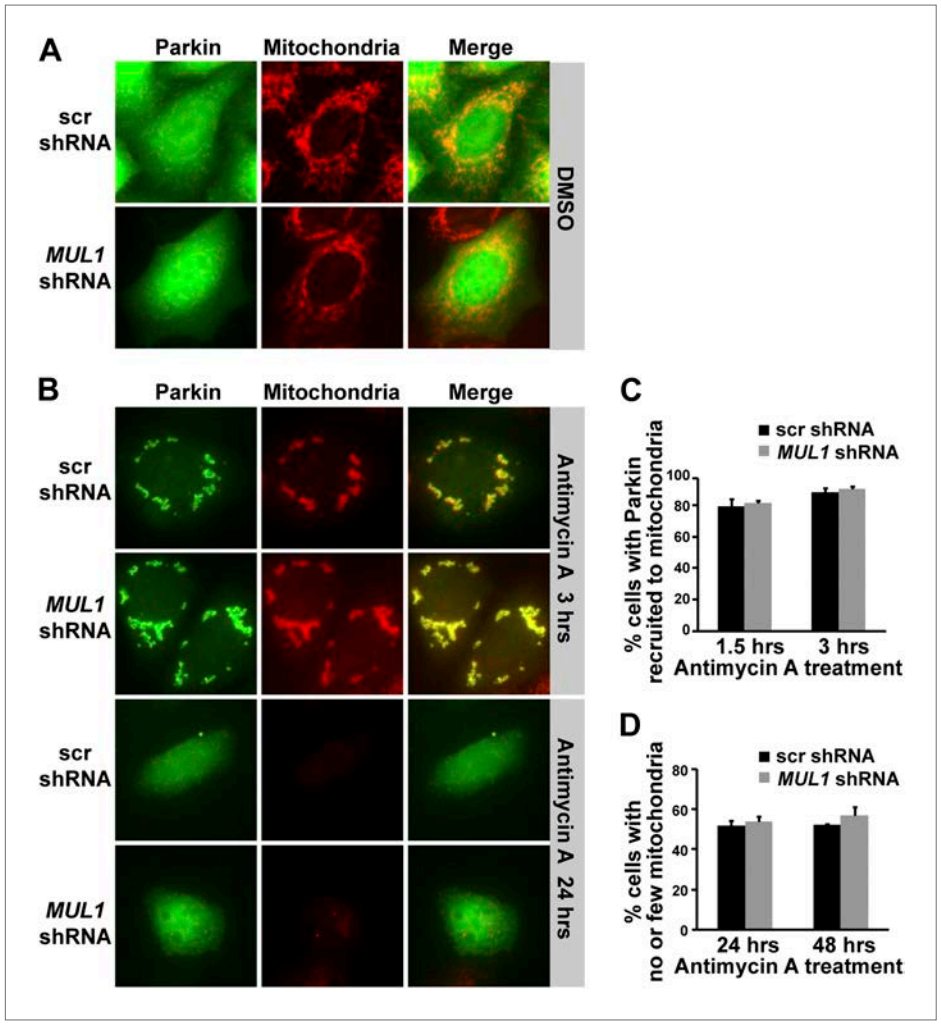

Figure 7—figure supplement 1. *MUL1* knockdown does not affect Parkin-mediated mitophagy.

DOI: 10.7554/eLife.01958.013

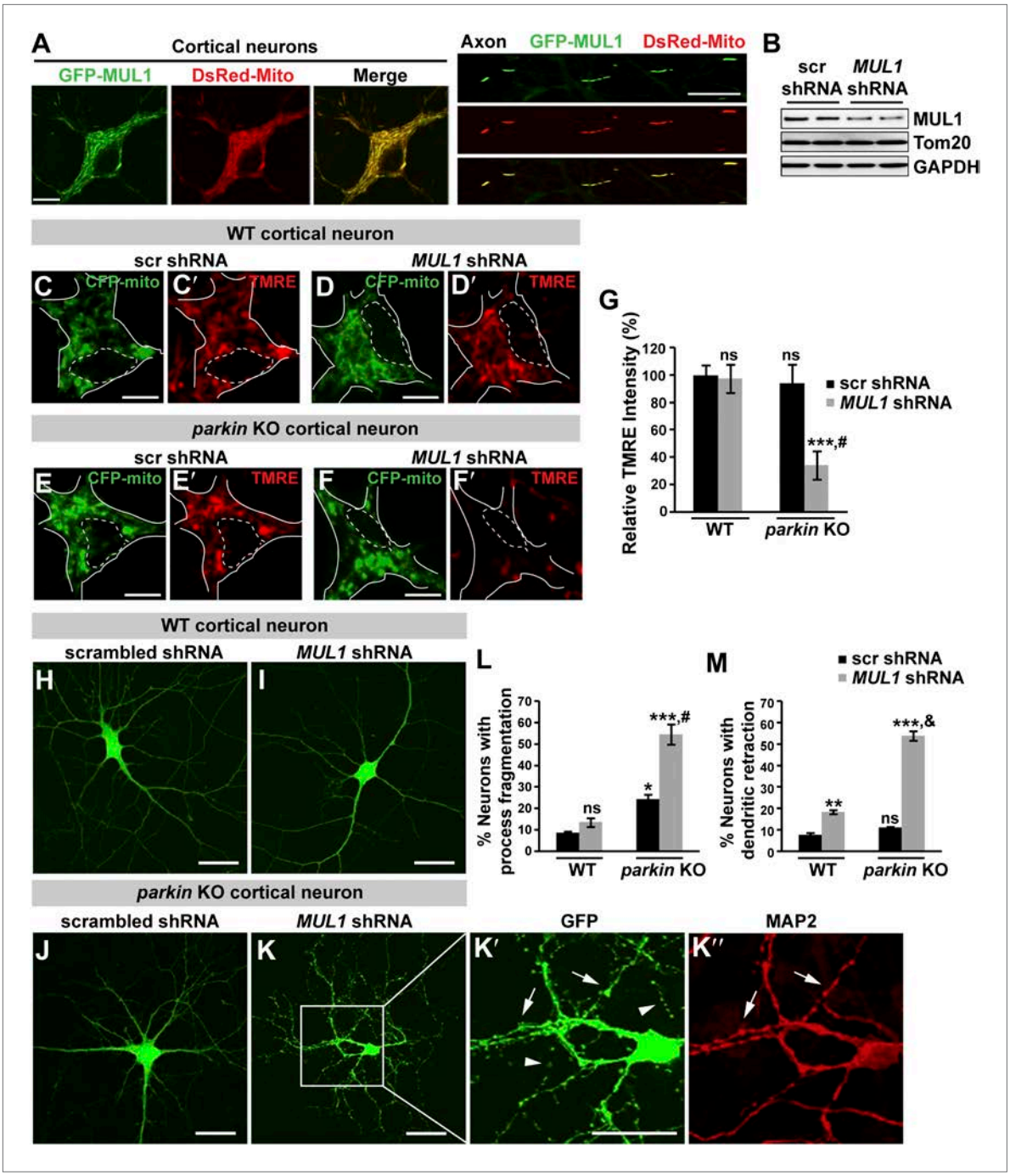

Figure 8. Loss of both *MUL1* and *parkin* aggravates mitochondrial damage and induces degeneration-like phenotypes in mouse cortical neurons. (**A**) MUL1 targets mitochondria in the cell bodies and axons of mouse primary cortical neurons. Neuronal mitochondria were labeled by DsRed-Mito or stained with an antibody against mitochondrial marker, TOM20 or Cytochrome C (***Figure 8—figure supplement 1***). (**B**) Levels of endogenous MUL1 in neurons transfected with scrambled or *MUL1* shRNA. Note that partial suppression of endogenous MUL1 may reflect relative low transfection rate (20%) in the neuronal culture. (**C**–**F**′) Mitochondria in live cortical neurons were co-labeled by expressing CFP-mito, which targets all mitochondria, and by loading fluorescent dye TMRE, which stains healthy mitochondria dependent upon membrane potential ($\Delta\psi_m$). Loading TMRE also labels mitochondria in glia in the culture. The edges of neuron cell bodies are marked with white solid lines, and the nuclei are outlined with white dashed lines. In contrast to other neurons, *parkin* knockout neurons with *MUL1* knockdown show reduced TMRE intensity (**F** and **F**′), indicating decreased $\Delta\psi_m$. Scale bars: 10 μm. (**G**) Quantification of relative TMRE intensity. TMRE intensity measured from each group of neurons was normalized to WT neurons transfected with scrambled shRNA. The data are shown as the means ± SEM from three experiments. (n ≥ 12 for each group). *** Significantly different from wild-type neurons transfected with scrambled shRNA, p<0.001. ns: not statistically significant (One-way ANOVA with Tukey's multiple

Figure 8. Continued on next page

Figure 8. Continued

comparisons test). # Significantly different from wild-type neurons transfected with *MUL1* shRNA and *parkin* KO neurons transfected with scrambled shRNA, p<0.001 and p<0.01, respectively (Two-way ANOVA with Tukey's multiple comparisons test). (**H**–**M**) *MUL1* knockdown in *parkin* KO neurons results in enhanced fragmentation of neurites. Representative wild-type (**H** and **I**) and *parkin* KO (**J**–**K**″) cortical neurons transfected with scrambled or *MUL1* shRNA and labeled with GFP (confirming transfection of shRNA and labeling axons and dendrites). (**K**′–**K**″) Higher magnification of a white box in **K** showing the soma and proximal dendrites labeled with an anti-MAP2 antibody (red). Arrows point to the GFP- and MAP2-labeled dendrites, and arrowheads indicate GFP-labeled but MAP2-negative fragmented axons. Scale bars: 20 μm. (**L** and **M**) Quantitative analysis showing enhanced process fragmentation (**L**) and dendritic retraction (**M**). The data are shown as the means ± SEM from three experiments (process fragmentation phenotype: n ≥ 115 for each genotype, dendritic retraction: n ≥ 127 for each phenotype). *, **, and *** Significantly different from wild-type neurons transfected with scrambled shRNA, p<0.05, p<0.01, and p<0.001, respectively. ns: not statistically significant (One-way ANOVA with Tukey's multiple comparisons test). # Significantly different from wild-type neurons transfected with *MUL1* shRNA and *parkin* KO neurons transfected with scrambled shRNA, both p<0.001. & Significantly different from wild-type neurons transfected with *MUL1* shRNA and *parkin* KO neurons transfected with scrambled shRNA, both p<0.001 (Two-way ANOVA with Tukey's multiple comparisons test).

DOI: 10.7554/eLife.01958.014

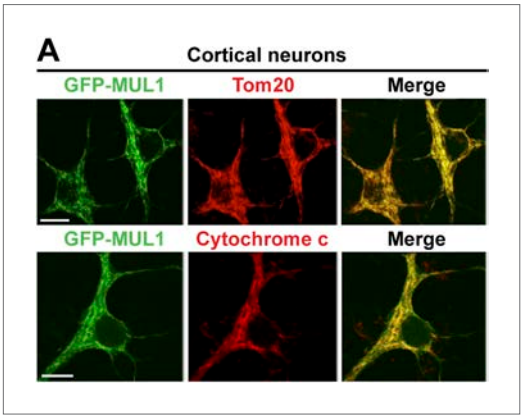

Figure 8—figure supplement 1. MUL1 localizes to mitochondria in mouse cortical neurons.

DOI: 10.7554/eLife.01958.015

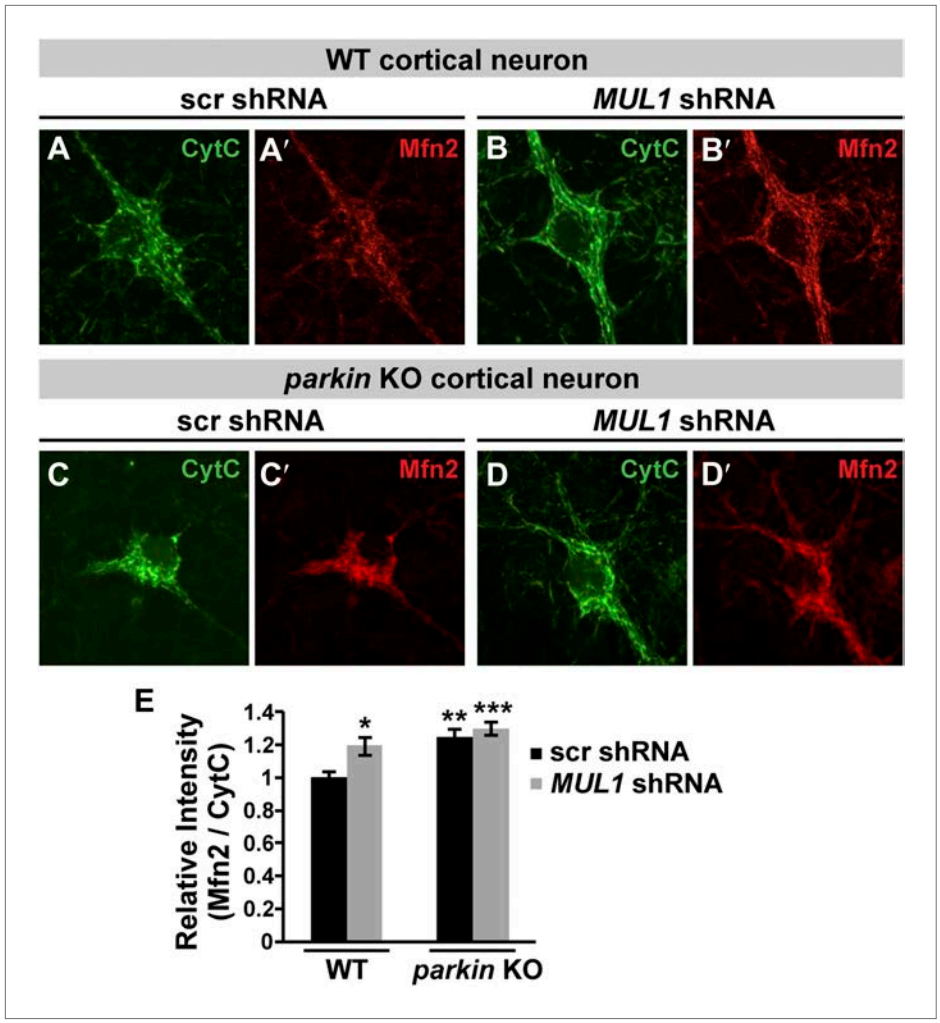

Figure 8—figure supplement 2. *MUL1* knockdown increases Mfn2 levels in mouse cortical neurons.
DOI: 10.7554/eLife.01958.016

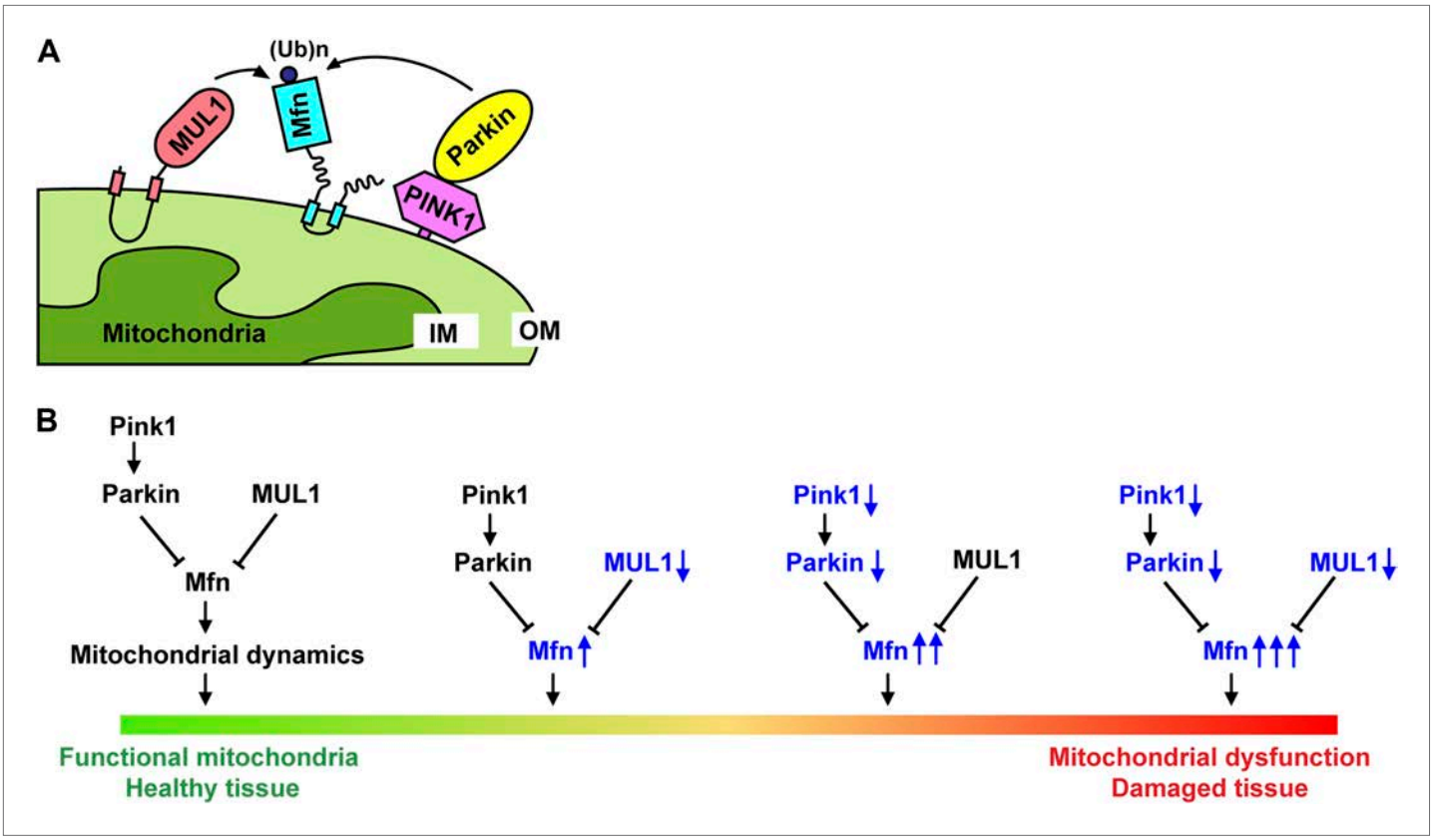

Figure 9. Models for how *MUL1* interacts with *PINK1/parkin*. (**A**) Schematic depictions of how MUL1, PINK1, Parkin, and Mfn interact in the mitochondria. In mammalian cells, upon mitochondrial damage (CCCP or antimycin A treatment), PINK1 is stabilized onto the mitochondrial OM of damaged mitochondria, with its kinase domain facing the cytosol (***Zhou et al., 2008***). PINK1 recruits Parkin onto the OM, either through direct phosphorylation or indirect interaction with other proteins (not depicted here) (***Jin and Youle, 2012***). Parkin then ubiquitinates multiple substrates on the OM, including Mfn. MUL1, a mitochondrial OM-anchored ligase with its RNF domain facing the cytosol, also mediates ubiquitination of Mitofusin. (**B**) The *PINK1/parkin* pathway and *MUL1* act in parallel to regulate *mfn*, and maintain mitochondrial function and tissue health. Reducing either *PINK1/parkin* or *MUL1* leads to increased levels of Mfn. Significant elevation of Mfn leads to mitochondrial dysfunction and tissue damage, similar to what is observed in *PINK1/parkin* mutants. Loss of both *PINK1/parkin* and *MUL1* leads to significantly higher Mfn levels, associated with severe mitochondrial dysfunction and tissue damage. OM: mitochondrial outer membrane; IM: mitochondrial inner membrane.

DOI: 10.7554/eLife.01958.017